Chin. Phys. B Vol. 29, No. 8 (2020) 080302

Quantum to classical transition induced by a classically small influence*

Wen-Lei Zhao(赵文垒)[1,†] and Quanlin Jie(揭泉林)[2]

[1] *School of Science, Jiangxi University of Science and Technology, Ganzhou* 341000, *China*
[2] *Department of Physics, Wuhan University, Wuhan* 430072, *China*

(Received 3 March 2020; revised manuscript received 7 April 2020; accepted manuscript online 17 April 2020)

We investigate the quantum to classical transition induced by two-particle interaction via a system of periodically kicked particles. The classical dynamics of particle 1 is almost unaffected in condition that its mass is much larger than that of particle 2. Interestingly, such classically weak influence leads to the quantum to classical transition of the dynamical behavior of particle 1. Namely, the quantum diffusion of this particle undergoes the transition from dynamical localization to the classically chaotic diffusion with the decrease of the effective Planck constant $\hbar_{\text{eff}}$. The behind physics is due to the growth of entanglement in the system. The classically very weak interaction leads to the exponential decay of purity in condition that the classical dynamics of external degrees freedom is strongly chaotic.

Keywords: quantum to classical transition, quantum decoherence, quantum chaos

PACS: 03.65.Ta, 05.45.−a, 05.45.Mt **DOI:** 10.1088/1674-1056/ab8a3a

1. Introduction

Rich dynamical behavior in periodically-driven systems has attracted extensive attention in recent years.[1–3] It is found that periodical driving induces quantized transport,[4,5] topological phase transition,[6–8] and thermalization of quantum dynamics,[9,10] just to name a few. Among these, the quantum transport in momentum space is particularly important, as it provides an insight on the mapping of transport phenomenon from position to momentum space. As an example, the dynamical localization (DL) in momentum space[11–13] is an analog of the Anderson localization in position space,[14] both of which result from the disordered feature of the system.[15] Nowadays, the transport phenomenon in momentum-space lattice has been a fruitful subject in physics, where the intriguing phenomena, such as topologically-protected quantum walk[16] and exponentially-fast diffusion[17–21] have been reported.

Theoretical investigations have stimulated experimental studies on the transport phenomenon in periodically-driven quantum systems. Recently, the DL was observed in the atom-optics experiments on the periodically-driven ultracold atoms[22] and molecules.[23] Even more remarkable, experimental advances in atom-optics have made it possible to actively tune the driven laser to be a quasiperiodic[24–26] or random sequence,[27] and thus to investigate the diffusion behavior in a controlled manner, e.g., the Anderson transition for the quasiperiodical kicking systems, and the decoherence-induced subdiffusion for the random kicking systems. These investigations greatly broaden our understanding on the exotic transport phenomenon induced by quantum coherence.[28–30]

It is known that the unavoidable coupling between system and environment destroys quantum coherence,[31] and consequently leads to the appearance of the classically chaotic diffusion from the underlying quantum dynamics.[32–41] Interestingly, the influence from a single chaotic particle can effectively produce the decoherence effects.[42–46] The quantum–classical correspondence (QCC) which is induced by the interaction with a few degrees of freedom[47–50] has been recently observed in a ultracold atoms experiment.[51] In the past decades, the influence of interatomic interactions on the quantum diffusion has received considerable investigations.[52–54] Rich diffusion behaviors, such as subdiffusion[55–61] and exponentially-fast diffusion,[18,19,21] have been observed. This topic regains attention as it is closely associated with the issue of dynamical many-body localization,[62–65] since the system of coupled periodically-kicking particles is an ideal system to explore the diffusion behavior in discrete momentum-space lattice.[66–69] At present, the fate of dynamical many-body localization under the interaction of particles is still an open question.[70]

Motivated by these studies, we investigate the quantum diffusion in a system involving two-coupled particles. The system is periodically driven by impulsive fields. We concentrate on both the classical and quantum dynamics of one particle (say particle 1) under the interaction with the other one (say particle 2). Interestingly, the effects of particle 2 with mass m on the classical diffusion of particle 1 with unity mass decrease as m decreases, and it is negligibly small when $m \ll 1$. The reason is that particle 2 of very small mass possesses little energy to affect the classical motion of particle 1. More im-

*Project supported by the National Natural Science Foundation of China (Grant Nos. 11864014 and 11804130).
†Corresponding author. E-mail: wlzhao@jxust.edu.cn
© 2020 Chinese Physical Society and IOP Publishing Ltd

portantly, the classically vanishing small influence is able to destroy the DL of particle 1. It even leads to the appearance of classically chaotic diffusion in quantum dynamics when the effective Planck constant $\hbar_{\rm eff}$ is small enough. To characterize the quantum entanglement, we numerically investigate the purity of the quantum state. The issue we address here is the sensitivity of entanglement to the classical chaoticity of the external degrees of freedom. We find that the time dependence of purity exhibits the power law decay for the regular motion of the classical dynamics of particle 2, and the exponential decay for the chaotic motion.

The paper is organized as follows. In Section 2, we describe the system and show the QCC of particle 1 subjected to the influence from a very small particle. In Section 3, we give a purity description of quantum entanglement. Summary is present in Section 4.

2. The quantum and classical diffusions

We consider two interacting particles which are trapped in an infinitely square well and periodically kicked by optical lattices. The Hamiltonian reads

$$H = H_1 + H_2 + H_{\rm I}\,, \tag{1}$$

where H_i $(i = 1,2)$ indicates the Hamiltonian of individual particles

$$H_i = \frac{p_i^2}{2m_i} + V_i\cos(2k_l x_i)\sum_n \delta(t - nT) + V(x_i)\,, \tag{2}$$

with $V(x_i)$ being an infinite square well

$$V(x_i) = \begin{cases} 0, & 0 < x_i < L, \\ +\infty, & \text{otherwise}, \end{cases} \tag{3}$$

and the interaction Hamiltonian $H_{\rm I}$ takes the form

$$H_{\rm I} = \varepsilon \exp\left[-\sigma(x_1 - x_2)^2\right]. \tag{4}$$

The variable p_i is the momentum, x_i is the coordinate, m_i is the mass of individual particles, k_l denotes the wave number, V_i is the amplitude of the kicking optical lattices with period T, and L is the width of the infinite square well. We consider the repulsive interaction for which the parameter σ is positive and the coupling strength is controlled by ε.

It is useful to introduce a set of scaled dimensionless units. Time is scaled by T, i.e., $t' = t/T$, which means that t' denotes the number of kicks. The canonical coordinate and momentum variables are redefined as $x_i' = 2k_l x_i$ and $p_i' = 2k_l T p_i/m_1$, which satisfy the commutation relation $[x_i', p_i'] = i\hbar_{\rm eff}$, with the effective Planck constant $\hbar_{\rm eff} = 4\hbar k_l^2 T/m_1$. The masses of the two particles are rescalled by m_1, thereby a dimensionless mass is $m = m_2/m_1$. The kicking strength in dimensionless units takes the form $K_i = V_i 4k_l^2 T^2/m_1$. For the interaction term, the scaled coupling strength is $\varepsilon = \varepsilon 4k_l^2 T^2/m_1$, and $\lambda = \sigma/4k_l^2$. The dimensionless width of the infinite square well has the expression $L' = 2k_l L$, For clarity, from here on, we omit the superscript of prime in these variables. After rescalling, the dimensionless Hamiltonian $\mathcal{H} = 4k_l^2 T^2/m_1 H$ is described as

$$\mathcal{H} = \mathcal{H}_1 + \mathcal{H}_2 + \mathcal{H}_{\rm I}\,, \tag{5}$$

where the Hamiltonian for the first particle is

$$\mathcal{H}_1 = \frac{p_1^2}{2} + V(x_1) + K_1\cos(x_1)\sum_n \delta(t - n)\,, \tag{6}$$

the Hamiltonian for the particle 2 is

$$\mathcal{H}_2 = \frac{p_2^2}{2m} + V(x_2) + K_1\cos(x_2)\sum_n \delta(t - n)\,, \tag{7}$$

and that for the interaction term takes the form

$$\mathcal{H}_{\rm I} = \varepsilon \exp\left[-\lambda(x_1 - x_2)^2\right]. \tag{8}$$

In this system, the mass of particle 1 is unity and that of particle 2 is a dimensionless quantity $m = m_2/m_1$ which can be adjusted by modifying m_1 and m_2. This opens the opportunity for investigating the dynamics of particle 1 under the influence of particle 2 with tunable mass.

We concentrate on both the classical and quantum dynamics of particle 1. Numerically, we use the split-operator method to simulate the time evolution of the quantum dynamics. The initial state is a product state of the ground state of each particle, i.e., $\psi(0) = \phi_1(0)\phi_2(0)$ with $\phi_i(0) = \sqrt{2/L}\sin(\pi x_i/L)$. The classical evolution of a trajectory is addressed by the fourth order Runge–Kutta Method. The initial condition of a trajectory (p_1, x_1, p_2, x_2) is such that the momentum of each particle is zero, $p_1 = p_2 = 0$, the coordinates x_1 and x_2 are uniformly distributed in the region $[0, L]$.

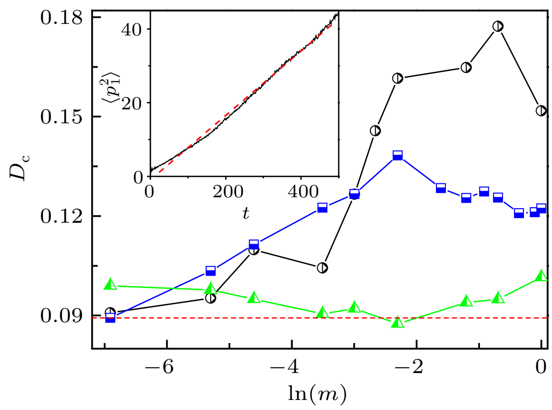

Fig. 1. Classical diffusion coefficient $D_{\rm c}$ of particle 1 versus m for $\varepsilon = 0.1$ (triangles), 2 (squares), and 4 (circles). The dashed line (in red) denotes the classical diffusion coefficient of unperturbed case, i.e., $\varepsilon = 0$. Inset: mean square of classical momentum of particle 1 versus time for $m = 0.001$. Dashed line (in red) denotes the fitting function of the form $\langle p_1^2(t) \rangle = D_{\rm c} t$ with $D_{\rm c} = 0.087$. The parameters are $K_1 = 1.8$, $K_2 = 0$, $\lambda = 10$, and $L = \pi$.

The typical character of classically chaotic diffusion is the linear growth of the mean energy with time, i.e., $\langle p^2(t)\rangle_c = D_c t$, where $\langle\cdots\rangle_c$ stands for the ensemble average over many trajectories and D_c is usually termed as the classical diffusion coefficient (CDC).[71–74] This phenomenon is traditionally referred as normal diffusion. Our numerical investigations show that the mean energy of particle 1 linearly increases with time $\langle p_1^2(t)\rangle_c = D_c t$ if the kick strength is strong enough (see the inset in Fig. 1). In our numerical simulations, the number of the classical trajectories is 10^4 and the evolution over one period is separated into 10^5 numbers of steps. In order to investigate the effects of particle 2 on the classical diffusion of particle 1, we numerically calculate the CDC of this particle, i.e., $D_c = \lim_{t_f\to\infty}\langle p_1^2(t_f)\rangle_c/t_f$ for different m. Here, t_f is the total time during which one may numerically track the time evolution. In our numerical experiments, t_f is on the scale of several hundreds of kicking periods, which can ensure the high precision of the numerical results due to the linear growth of mean energy with time. Interestingly, with the decrease of m, D_c decreases to the saturation level which almost equals with the CDC of the unperturbed case (see Fig. 1 for $\varepsilon = 2$ and 4). This demonstrates that the influence from particle 2 decreases as m decreases and it is even negligible if $m \ll 1$. For weak coupling (e.g., $\varepsilon = 0.1$), the D_c of particle 1 has slight difference from that of the unperturbed case as m varies, since the two particles have little effects on each other for very weak coupling.

We numerically investigate the quantum diffusion of particle 1 when its classical counterpart is almost unaffected which is ensured by the condition $m \ll 1$. The quantum mean energy $\langle p_1^2(t)\rangle_q$ of this subsystem exhibits DL for large $\hbar_{\text{eff}}$ [e.g., $\hbar_{\text{eff}} = 0.05$ in Fig. 2(a)]. Interestingly, the quantum diffusion of particle 1 undergoes the transition from DL to classically-chaotic diffusion as $\hbar_{\text{eff}}$ decreases. For small enough $\hbar_{\text{eff}}$ (e.g., for $\hbar_{\text{eff}} = 0.01$), the quantum diffusion is in good agreement with its classical counterpart, which is a clear evidence of QCC. At first glance, such QCC happening for very small $\hbar_{\text{eff}}$ is trivial. However, by comparing with the quantum mean energy with $\varepsilon = 0$, one can find that the quantum diffusion of the unperturbed case is eventually suppressed by quantum coherence after long time evolution [see Fig. 2(a) for $\hbar_{\text{eff}} = 0.01$]. Therefore, the interaction plays a key role for the appearance of QCC. To reveal rich features of quantum diffusion, we numerically investigate the probability density distribution in momentum space. Our numerical results show that for large $\hbar_{\text{eff}}$ [e.g., $\hbar_{\text{eff}} = 0.05$ in Fig. 2(b)], the wave packet is exponentially localized in momentum space, which is a feature of DL. For small enough $\hbar_{\text{eff}}$ [e.g., $\hbar_{\text{eff}} = 0.01$ in Fig. 2(b)], the momentum distribution is in a good agreement with the Gaussian function, which is a signature of the appearance classically chaotic diffusion. The change from the exponentially-localized profile of wavepackets to the Gaussian form reveals the quantum to classical transition.

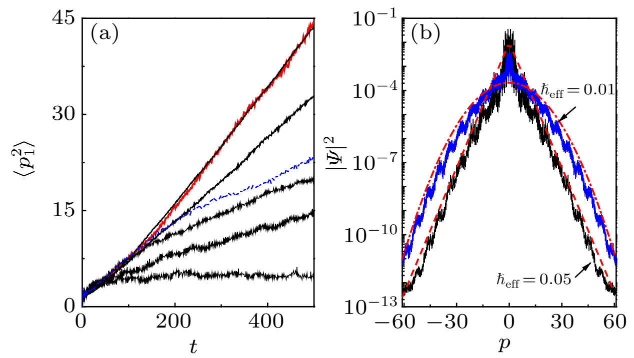

Fig. 2. (a) Time dependence of the classical (red line) mean energy and quantum mean energy (black lines) of particle 1. From top to bottom, black solid lines correspond to $\hbar_{\text{eff}} = 0.01$, 0.02, 0.03, 0.04, and 0.05, respectively. The parameters are $K_1 = 1.8$, $K_2 = 0$, $m = 0.001$, $\varepsilon = 2$, $\lambda = 10$, and $L = \pi$. For comparison, the dashed line (in blue) denotes the quantum mean energy of the unperturbed case, i.e., $\varepsilon = 0$ with $K = 1.8$ and $\hbar_{\text{eff}} = 0.01$. (b) Momentum distribution at the time $t = 500$ with $\hbar_{\text{eff}} = 0.01$ (blue curve) and 0.05 (black curve). Dash-dotted line (in red) indicates the fitting function of the Gaussian form $|\psi_1(p)|^2 \propto e^{-p^2/\zeta}$. Dashed line (in red) denotes the exponential fitting $|\psi_1(p)|^2 \propto e^{-|p|/\xi}$.

In chaotic situation, the motion of particle 2 of very small mass behaves like random noise. It is known that external noises can destroy quantum interference and thus leads to the classically chaotic diffusion.[75–77] As a further step, we consider the case that the kick strength contains random noises, for which the Hamiltonian reads

$$H = \frac{p^2}{2} + (K + \delta_K)\cos(x)\sum_n \delta(t-n) + V(x)\,, \qquad (9)$$

where δ_K is random numbers uniformly distributed in the interval $[0, \delta_K^{\max}]$, and $V(x)$ denotes an infinite square well. We numerically investigate the quantum diffusion for different $\delta_K^{\max}$. In numerical simulations, we take the average of the expectation value $\langle p^2\rangle$ over 50 realizations of random δ_K to reduce the fluctuations of the time dependence of the physical observable. Our numerical results show that for a specific $\hbar_{\text{eff}}$ the quantum diffusion exhibits the transition from DL to the classically chaotic diffusion with the increase of $\delta_K^{\max}$, as shown in Fig. 3(a). Note that the strength of the random noise is much smaller than that of the kick strength, i.e., $\delta_K^{\max} \ll K$, thus the chaotic diffusion emerging from quantum dynamics with $\delta_K^{\max}$ is in good consistence with the classically normal diffusion of the unperturbed case. In the presence of random noise, the quantum diffusion also undergoes the quantum to classical transition with the decrease of $\hbar_{\text{eff}}$ [see Fig. 3(b) for $\delta_K^{\max} = 0.012$]. The comparison of the quantum states between the random kicking system with $\delta_K^{\max} = 0.012$ and the two-particle system with $m = 0.001$ shows the good agreement both for DL and chaotic diffusion, as shown in Fig. 3(c). It is therefore reasonable to believe that the influence from a small particle resembles random noises on the system.

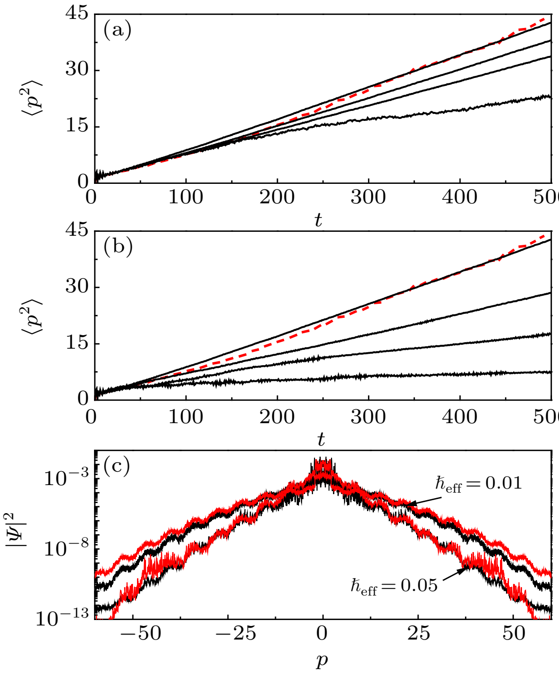

Fig. 3. (a), (b) Time dependence of the mean energy. In (a), $\hbar_{\rm eff}=0.01$, from top to bottom solid lines correspond to $\delta_K^{\max}=0.012$, 0.008, 0.005, and 0. In (b), $\delta_K^{\max}=0.012$, from top to bottom solid lines correspond to $\hbar_{\rm eff}=0.01$, 0.02, 0.03, and 0.05. For comparison, red-dashed lines denote the classical mean energy with $\delta_K^{\max}=0$. (c) Momentum distribution at the time $t=500$ with $\delta_K^{\max}=0.012$ for $\hbar_{\rm eff}=0.01$ and 0.05, respectively. The parameters are $K=1.8$ and $L=\pi$. Black curves denote the momentum distributions for the two-particle systems with $m=0.001$, $K_1=1.8$, $\varepsilon=2$, $\lambda=10$, and $L=\pi$ (same as in Fig. 1(b)).

We quantify the difference between quantum and diffusion coefficients of particle 1 by using the ratio $\mathcal{R}=D_{\rm q}/D_{\rm c}$, where the quantum diffusion coefficient is defined as $D_{\rm q}=\lim_{t_{\rm f}\to\infty}\langle p_1^2(t_{\rm f})\rangle_{\rm q}/t_{\rm f}$. In the ideal case, the DL ($D_{\rm q}=0$) and QCC ($D_{\rm q}=D_{\rm c}$) correspond to $\mathcal{R}=0$ and 1, respectively. In numerical simulations, we evolve the system for 500 periods to calculate both $D_{\rm c}$ and $D_{\rm q}$, and thus obtain the value $\mathcal{R}$. Figure 4(a) shows the dependence of $\mathcal{R}$ on $\hbar_{\rm eff}$ for various m. It is seen that with increasing $\hbar_{\rm eff}$, the $\mathcal{R}$ exponentially decays as $\mathcal{R}\propto {\rm e}^{-\alpha\hbar_{\rm eff}}$ from almost unity to the saturation level which is around $\mathcal{R}=0.1$. This clearly demonstrates the exponentially-fast departure of the quantum dynamics from its classical limit. Note that the saturation region of $\mathcal{R}\approx 0.1$ indicates the appearance of DL. Due to the finite time evolution in numerical simulations, the value of $D_{\rm q}$ for DL is not exactly zero, which results in the saturation of $\mathcal{R}\approx 0.1$. Detailed observations show that the decay rate α of $\mathcal{R}$ increases with the decrease of m, which reveals that the quantum dynamics of particle 1 is much easier to deviate from its classical counterpart if the mass of particle 2 gets smaller. This is due to the fact that the influence from particle 2 on particle 1 decreases as m decreases.

Furthermore, we define the criteria of the appearance of the classically chaotic diffusion and DL as $\mathcal{R}=0.9$ and 0.1, respectively. We numerically obtain the threshold values of $\hbar_{\rm eff}$ corresponding to $\mathcal{R}=0.9$ and 0.1, which are separately termed as $\hbar_{\rm eff}^{\rm c}$ and $\hbar_{\rm eff}^{\rm d}$. The dependence of $\hbar_{\rm eff}^{\rm c}$ and $\hbar_{\rm eff}^{\rm d}$ on m is depicted in Fig. 4(b). One can find three different regions in the parameter space $(\hbar,m)$. Blow the curve of $\hbar_{\rm eff}^{\rm c}$, there is the zone of QCC for which the quantum system exhibits chaotic diffusion. Above the curve $\hbar_{\rm eff}^{\rm d}$, the quantum system exhibits the DL since $\hbar_{\rm eff}$ is so large that the the quantum coherence is not destroyed by the interaction. There is a transition region between the classically chaotic diffusion zone and the DL zone. Our numerical result is useful for guiding the investigation on the diffusion behavior in cold-atom experiments.

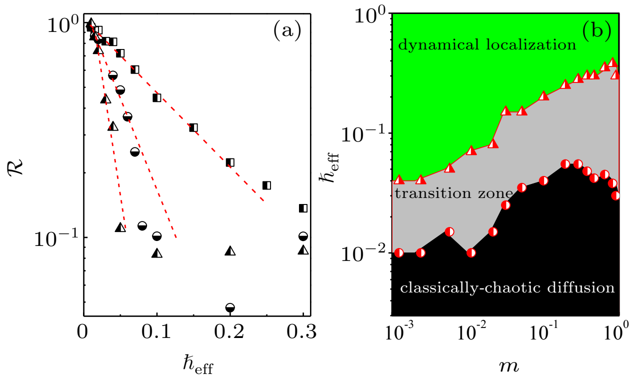

Fig. 4. (a) The ratio $\mathcal{R}$ versus $\hbar_{\rm eff}$ with $m=0.001$ (triangles), 0.01 (circles), and 1 (squares). Dashed lines (in red) denote the exponential fitting, i.e., $\mathcal{R}\propto {\rm e}^{-\alpha\hbar_{\rm eff}}$. (b) Phase diagram of quantum diffusion as a function of $\hbar_{\rm eff}$ and m, where circles and triangles indicate the threshold values of $\hbar_{\rm eff}^{\rm c}$ and $\hbar_{\rm eff}^{\rm d}$ which correspond to the appearance of classically chaotic diffusion and dynamical localization, respectively. The coupling strength is $\varepsilon=2$. Other parameters are the same as those in Fig. 2.

3. A purity description of entanglement

A commonly used measure of quantum entanglement is purity $\mathcal{P}={\rm Tr}(\rho_1^2)$, where ρ_1 is the reduced density matrix of particle 1 by tracing out the degree of particle 2 from the density matrix of the two-particle system.[78,79] The sensitivity of the quantum entanglement to external perturbations has been extensively studied in the context of quantum chaos.[80–82] In the present work, we numerically investigate the effects of the classically chaotic dynamics of particle 2 on the generation of quantum entanglement. We consider the case that the coupling strength is in the form $\varepsilon=\tilde{\varepsilon}\hbar_{\rm eff}$, for which the coupling is almost negligible in the semiclassical limit $\hbar_{\rm eff}\ll 1$. Our numerical results show that for small K_2, the purity decays in the power law of time, i.e., $\mathcal{P}\propto t^{-\eta}$ (see Fig. 5). For strong kick strength (e.g. $K_2=0.09$ and 0.12), the purity decays exponentially fast with time, i.e., $\mathcal{P}\propto\exp(-\gamma t)$. Moreover, the time-dependence of purity is almost unchanged as long as the K_2 is sufficiently strong. Our numerical result demonstrates that there is a regime where the exponentially-fast growth of entanglement is stable provided that the chaoticity of the external degree of freedom is strong enough.

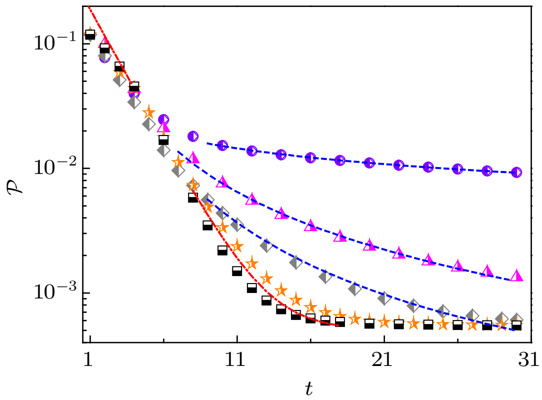

Fig. 5. Purity $\mathcal{P}$ versus time with $K_2 = 0$ (circles), 0.03 (triangles), 0.05 (diamonds), 0.09 (pentagrams), and 0.12 (squares). Dashed lines (in blue) denote the fitting function of the form $\mathcal{P} \propto t^{-\eta}$. Dashed-dotted (in red) line indicates the exponential fitting $\mathcal{P} \propto \exp(-\gamma t)$. The parameters are $K_1 = 5$, $m = 0.01$, $\hbar = 10^{-4}$, $\varepsilon = 20\hbar_{\text{eff}}$, $\lambda = 10$, and $L = \pi$.

4. Summary

We numerically investigate the entanglement involving a few degrees of freedom via two coupled particles. We show that, the effect of particle 2 on the classical behavior of particle 1 decreases as its mass (m) decreases. Under the classically weak perturbation ($m \ll 1$), the quantum diffusion behavior of particle 1 undergoes a transition from DL to chaotic diffusion with the decrease of $\hbar_{\text{eff}}$. We numerically investigate the difference between quantum and classical diffusions for a wide regime of $\hbar_{\text{eff}}$ and m, and find the exponential decay of $\mathcal{R}$ with $\hbar_{\text{eff}}$. By using this quantity, we define the boundary for the appearance of DL and classically-chaotic diffusion. Numerically, we obtain a "phase" diagram of the quantum diffusion in the parameters space $(\hbar_{\text{eff}}, m)$. The quantum to classical transition is accompanied by the growth of entanglement. For the vanishingly small interaction $\varepsilon \propto \hbar_{\text{eff}}$ with $\hbar_{\text{eff}} \ll 1$, the time decay of purity is exponentially fast in condition that the classical dynamics of particle 2 is strongly chaotic. Such exponentially-fast entanglement is stable in the sense that the time dependence of purity is almost unchanged as K_2 varies. Our investigation has important implication for the fundamental problem of the quantum to classical transition.

References

[1] Dana I 2014 *Phys. Rev. B* **89** 205111
[2] Ben-Harush M and Dana I 2016 *Phys. Rev. E* **93** 052207
[3] Wang J and Gong J B 2009 *Phys. Rev. Lett.* **102** 244102
[4] Ho D Y H and Gong J B 2012 *Phys. Rev. Lett.* **109** 010601
[5] Zhao W L, Wang J Z, Wang X H and Tong P Q 2019 *Phys. Rev. E* **99** 042201
[6] Zhou L W, Chen C and Gong J B 2016 *Phys. Rev. B* **94** 075443
[7] Li Z, Wang H Q, Zhang D W, Zhu S L and Xing D Y 2016 *Phys. Rev. A* **94** 043617
[8] Zhou L W and Gong J B 2018 *Phys. Rev. A* **97** 063603
[9] Borgonovi F, Izrailev F M, Santos L F and Zelevinsky V G 2016 *Phys. Rep.* **626** 1
[10] Neill C, Roushan P, Fang M, *et al.*, 2016 *Nat. Phys.* **12** 1037
[11] Casati G, Chirikov B V, Izraelev F M and Ford J 1979 *Stochastic Behavior in Classical and Quantum Hamiltonian Systems, Lecture Notes in Physics* (Berlin: Springer) p. 334
[12] Izrailev F M 1990 *Phys. Rep.* **196** 299
[13] Dana I 2014 *Can. J. Chem.* **92** 77
[14] Anderson P W 1958 *Phys. Rev.* **109** 1492
[15] Fishman S, Grempel D R and Prange R E 1982 *Phys. Rev. Lett.* **49** 509
[16] Dadras S, Gresch A, Groiseau C, Wimberger S and Summy G S 2018 *Phys. Rev. Lett.* **121** 070402
[17] Wang J, Guarneri I, Casati G and Gong J B 2011 *Phys. Rev. Lett.* **107** 234104
[18] Mieck B and Graham G 2005 *J. Phys. A: Math. Gen.* **38** L139
[19] Zhao W L, Gong J B, Wang W G, Casati G, Liu J and Fu L B 2016 *Phys. Rev. A* **94** 053631
[20] Zhao W L, Wang J Z and Wang W G 2019 *J. Phys. A: Math. Theor.* **52** 305101
[21] Guarneri I 2017 *Phys. Rev. E* **95** 032206
[22] Lopez M, Clement J F, Szriftgiser P, Garreau J C and Delande D 2012 *Phys. Rev. Lett.* **108** 095701
[23] Bitter M and Milner V 2017 *Phys. Rev. Lett.* **118** 034101
[24] Chabé J, Lemarie G, Gremaud B, Delande D, Szriftgiser P and Garreau J C 2008 *Phys. Rev. Lett.* **101** 255702
[25] Lemarié G, Chabé J, Szriftgiser P, Garreau J C, Grémaud B and Delande D 2009 *Phys. Rev. A* **80** 043626
[26] Garreau J C 2017 *C. R. Phys.* **18** 31
[27] Sarkar S, Paul S, Vishwakarma C, Kumar S, Verma G, Sainath S, Rapol U D and Santhanam M S 2017 *Phys. Rev. Lett.* **118** 174101
[28] Hainaut C, Manai I, Chicireanu R, Clément J, Zemmouri S and Garreau J C 2017 *Phys. Rev. Lett.* **118** 184101
[29] Tan J T, Luo Y R, Zhou Z and Hai W H 2016 *Chin. Phys. Lett. bf* **33** 070302
[30] Li Z, Wang J Z and Fu L B 2013 *Chin. Phys. Lett.* **30** 010301
[31] Yang Y B and Wang W G 2015 *Chin. Phys. Lett.* **32** 030301
[32] Joos E, Zeh H D, Kiefer C, Giulini D, Kupsch J and Stamatescu I O 2003 *Decoherence and the Appearance of a Classical World in Quantum Theory* (Berlin: Springer) p. 41
[33] Zurek W H 2003 *Rev. Mod. Phys.* **75** 715
[34] Schlosshauer M 2004 *Rev. Mod. Phys.* **76** 1267
[35] Schlosshauer M 2008 *Found. Phys.* **38** 796
[36] Chaudhry A Z and Gong J B 2014 *Phys. Rev. A* **89** 014104
[37] Wang W G, He L W and Gong J B 2012 *Phys. Rev. Lett.* **108** 070403
[38] Feynman R P and Vernon F L 1963 *Ann. Phys. (Leipzig)* **24** 118
[39] Caldeira A O and Leggett A J 1983 *Physica (Amsterdam)* **121**A 587
[40] Wisniacki D and Toscano F 2009 *Phys. Rev. E* **79** 025203(R)
[41] Petitjean C and Jacquod P 2006 *Phys. Rev. Lett.* **97** 194103
[42] Rossini D, Benenti G and Casati G 2006 *Phys. Rev. E* **74** 036209
[43] Bandyopadhyay J N 2009 *Europhys. Lett.* **85** 50006
[44] Adachi S, Toda M and Ikeda K 1988 *Phys. Rev. Lett.* **61** 659
[45] Graham R and Kolovsky A R 1996 *Phys. Rev. A* **222** 47
[46] Park H K and Kim S W 2003 *Phys. Rev. A* **67** 060102(R)
[47] Takahashi K 1989 *Prog. Theor. Phys. Suppl.* **98** 109
[48] Zhao W L and Jie Q L 2009 *Commun. Theor. Phys.* **51** 465
[49] Zhao W L, Jie Q L and Zhou B 2010 *Commun. Theor. Phys.* **54** 247
[50] Zhao W L, Wang J Z and Dou F Q 2012 *Acta Phys. Sin.* **61** 240302 (in China)
[51] Gadway B, Reeves J, Krinner L and Schneble D 2013 *Phys. Rev. Lett.* **110** 190401
[52] Shepelyansky D L 1994 *Phys. Rev. Lett.* **73** 2607
[53] Borgonovi F and Shepelyansky D L 1995 *Nonlinearity* **8** 877
[54] Qin P Q, Andreanov A, Park H C and Flach S 2017 *Sci. Rep.* **7** 41139
[55] Shepelyansky D L 1993 *Phys. Rev. Lett.* **70** 1787
[56] García-Mata I and Shepelyansky D L 2009 *Phys. Rev. E* **79** 026205
[57] Flach S, Krimer D O and Skokos C 2009 *Phys. Rev. E* **79** 026205
[58] Veksler H, Krivolapov Y and Fishman S 2009 *Phys. Rev. E* **80** 037201
[59] Pikovsky A and Fishman S 2011 *Phys. Rev. E* **83** 025201
[60] Michaely E and Fishman S 2012 *Phys. Rev. E* **85** 046218
[61] Fishman S, Krivolapov Y and Soffer A 2012 *Nonlinearity* **25** 53
[62] Rozenbaum E B and Galitski V 2017 *Phys. Rev. B* **95** 064303
[63] Notarnicola S, Iemini F, Rossini D, Fazio R, Silva A and Russomanno A 2018 *Phys. Rev. E* **97** 022202
[64] Keser A C, Ganeshan S, Refael G and Galitski V 2016 *Phys. Rev. B* **94** 085120
[65] Čadež T, Mondaini R and Sacramento P D 2017 *Phys. Rev. B* **96** 144301
[66] Gadway B 2015 *Phys. Rev. A* **92** 043606

[67] Alex An F, Meier E J, Ang'ong'a J and Gadway B 2018 *Phys. Rev. Lett.* **120** 040407
[68] Alex An F, Meier E J and Gadway B 2017 *Nat. Comm* **8** 325
[69] Meier E J, Alex An F and Gadway B 2016 *Phys. Rev. A* **93** 051602(R)
[70] Abanin D A, Roeck W D and Huveneers F 2015 *Phys. Rev. Lett.* **115** 256803
[71] Hu B, Li B W, Liu J and Gu Y 1999 *Phys. Rev. Lett.* **82** 4224
[72] Liu J, Cheng W T and Cheng C G 2000 *Commun. Theor. Phys.* **33** 15
[73] Chen H S, Wang J and Gu Y 2000 *Chin. Phys. Lett.* **17** 85
[74] Paul S, Pal H and Santhanam M S 2016 *Phys. Rev. A* **93** 060203(R)
[75] Milner V, Steck D A, Oskay W H and Raizen M G 2000 *Phys. Rev. E.* **61** 7223
[76] Karney C F F, Rechester A B and White R B 1982 *Physica D* **3** 425
[77] Ott E, Antonsen T M, Jr and Hanson J D 1984 *Phys. Rev. Lett.* **53** 2187
[78] Lakshminarayan A 2001 *Phys. Rev. E* **64** 036207
[79] Bandyopadhyay J N and Lakshminarayan A 2002 *Phys. Rev. A* **89** 060402
[80] Cohen D and Heller E J 2000 *Phys. Rev. Lett.* **84** 2841
[81] Wisniacki D A and Cohen D 2002 *Phys. Rev. E* **66** 046209
[82] Wisniacki D A, Ares N and Vergini E G 2010 *Phys. Rev. Lett.* **104** 254101